

## Characterization of a Dielectric Barrier Discharge in axisymmetric and planar configurations -Electrical Properties-

Boni Dramane, Nouredine Zouzou, Eric Moreau and Gerard Touchard

Laboratoire d'Etudes Aérodynamiques (LEA), Université de Poitiers, ENSMA, CNRS  
2 Bd. Marie & Pierre Curie, Téléport 2, BP. 30179, 86962, Futuroscope Chasseneuil Cedex, France

**Abstract**— The characteristics of a Dielectric Barrier Discharge (DBD) in axisymmetric and planar configurations are studied and compared by measuring their electrical discharge parameters and the airflow influence on these parameters. With the axisymmetric reactor, the application of AC high voltage generates a stable and quasi-diffuse discharge whereas the planar reactor generates a filamentary and unstable discharge. When the flow rate increases the discharge current and the electric power decrease in both cases. This effect is less pronounced in the planar configuration.

**Keywords**— Dielectric barrier discharge, Wire to cylinder reactor, Plane to plane reactor

### I. INTRODUCTION

Dielectric Barrier Discharge (DBD) is well known to produce highly non-equilibrium plasmas in a controllable way at atmospheric pressure. This method can effectively generate atoms, radicals, and excited species with energetic electrons at moderate gas temperatures [1, 2].

Because of its high electron density and energy, the DBD in air has been used to clean hazardous air pollutants (HAPs) [3-5].

In general, operating at atmospheric pressure, the DBD is generated in filamentary form [6]. DBDs can also be obtained in a diffuse form under certain configurations and conditions [7-9].

In order to remove ultra fine particles from Diesel exhaust, two DBD reactors have been used to determine which of them gives the lowest energy density for an efficient removal. The reactors are in axisymmetric and planar configurations.

This preliminary study was performed by measuring the electrical parameters of the discharge: applied voltage, discharge current, transferred charge, and electric power consumption. The results obtained in both configurations were compared. A detailed attention was given to the influence of the flow on the discharge behavior.

### II. EXPERIMENTAL

In order to determine which type of configuration will make it possible to obtain a diffuse discharge or rather a filament discharge, we used two types of reactor in different configurations.

Figure 1 shows a schematic illustration of the axisymmetric reactor used in this work, while figure 2 shows the planar one.

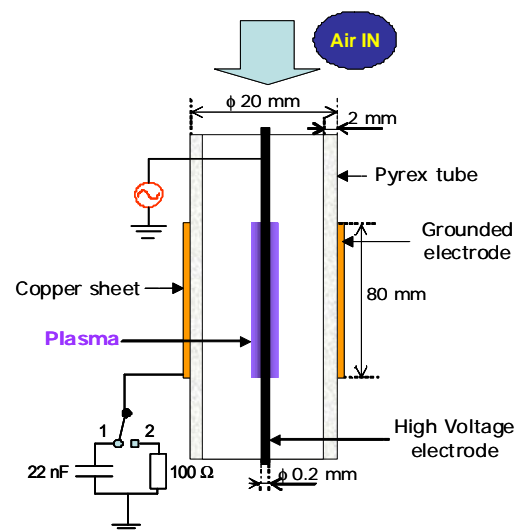


Fig. 1. Schematic of the axisymmetric reactor

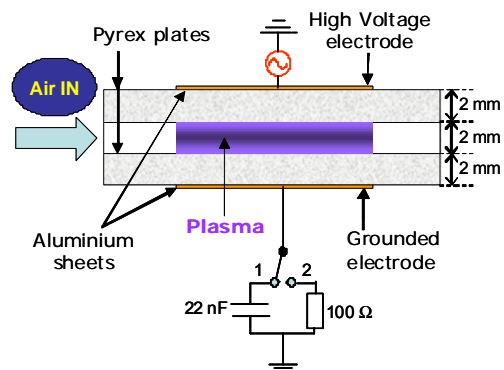


Fig. 2. Schematic of the planar reactor.

Corresponding author: Boni Dramane  
e-mail address: boni.dramane@lea.univ-poitiers.fr

Received: July 10th, 2007, Revised: March 12th, 2008, Accepted: March 30th, 2008

The axisymmetric configuration setup consists of a Pyrex tube, a copper sheet, a stainless wire and an air circulation system. Outer diameter of the Pyrex tube was 20 mm and the thickness was 2 mm. The copper sheet with 8 cm width was rolled up on the outer surface of the Pyrex tube. The stainless wire of 0.2 mm of diameter was maintained tended on the central axis of the tube and connected to the high voltage.

The planar configuration setup consists of two aluminum sheets, two plates made of Pyrex and an air circulation system. With a thickness of 0.1 mm and an area of  $50 \times 47 \text{ mm}^2$ , each aluminum foil is stuck on the dielectric plate. Using spacers made of glass of 2 mm thick, the active volume of the discharge was  $50 \times 40 \times 2 \text{ mm}^3$ . The top sheet, used as the active electrode, was connected to high voltage and the bottom one was grounded. To avoid the edge effect, the electrode contours were encapsulated in epoxy resin.

The high voltage power amplifier (Trek, 20/20C,  $\pm 20 \text{ kV} / \pm 20 \text{ mA}$ ) was driven by a function generator (HAMEG, HM8130) to generate high voltage sine wave. High voltage up to 20 kV was applied to the high voltage electrode with frequencies of 0.5, 1 and 2 kHz. Applied voltage was monitored with an oscilloscope (Tektronix, TDS3014B) with a high voltage divider (Lecroy 1000:1, 20 kV). The total current of discharge is measured with a resistor of  $100 \ \Omega$  and the transferred charge with a capacitor of 22 nF.

All the experiments were carried out under atmospheric pressure at room temperature. The airflow inside the reactors was controlled. The flow rate ( $Q$ ) is measured with a flow meter (Brooks, tube size R-6-15-A, Tantalum ball).

### III. RESULTS AND DISCUSSION

#### A. Discharge characteristics in each configuration

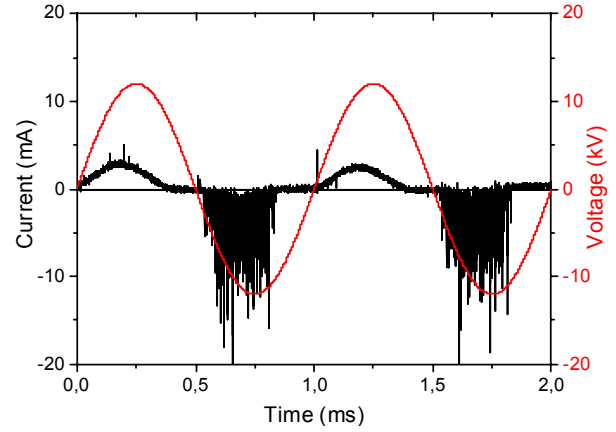
Typical oscillograms of the applied voltage, discharge current, transferred charge and charge-voltage curve in the Lissajous figure with axisymmetric and planar reactors are shown in figures 3 and 4, respectively.

Figure 3- a shows the time evolution of the applied voltage and the discharge current obtained from the measured current. Indeed, the measured current includes fast component (current pulse) and slow component (capacitive and pseudo continuous current). The capacitive current, which was estimated from the  $I-t$  curve with applied voltage low enough to generate any discharge, was subtracted from the measured current to obtain the discharge current. All the discharge currents hereafter are presented in this way.

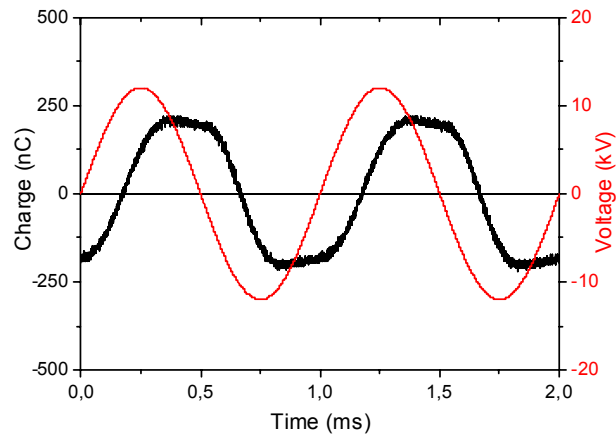
The discharge current waveform shows only few pulses of current on the positive half-cycle, while on the negative one the number of pulses is significant. In the positive half-cycle of the applied voltage, the plasma is characterized by a glow-like type. However, the Trichel

pulses dominate the negative half-cycle. This behavior is also observed in point to plane DBD [10].

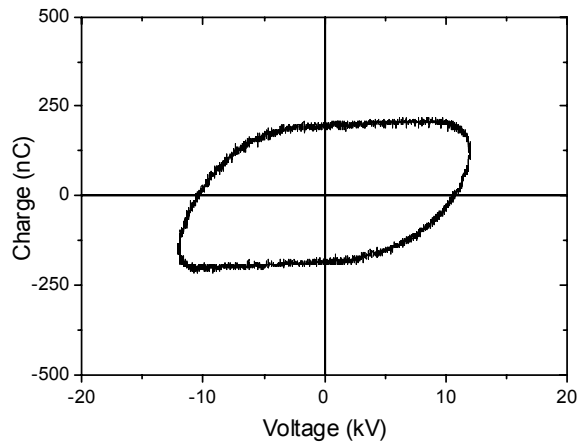
The transferred charge waveform shown in figure 3- b presents an evolution which can be break up into two steps. During the positive half-cycle, the transferred charge increases and after the voltage maximum it



(a)



(b)



(c)

Fig. 3. Axisymmetric reactor characteristics: (a) time evolution of the discharge current, (b) time evolution of the transferred charge, and (c) charge-voltage curve. Conditions:  $V_{\text{peak}} = 12 \text{ kV}$ ;  $f = 1 \text{ kHz}$ ;  $Q = 4.7 \text{ L.min}^{-1}$ .

stabilizes. The transferred charge decreases again for another sequence.

The charge-voltage curve (figure 3- c) represents a close loop, which will be described in the following section.

In contrast, the discharge in planar configuration is characterized by a filamentary behavior (figure 4- a). The current pulses are higher in magnitude and less numerous during the positive half-cycle than on the negative one.

The time evolution of the transferred charge shows similar steps as that found in axisymmetric configuration (figure 4- b).

Another difference between both configurations is their charge-voltage curve. It is noted that, in opposition to the planar configuration, with a figure close to a parallelogram [3], the charge-voltage curve in axisymmetric configuration shows a kind of ring of the shape of an ellipse flattened on the edges.

The slope of the curve represents the total capacitance ( $C_{tot}$ ) of the reactor [11]. Indeed, the total capacitance of the reactors without discharge is  $1/C_{tot}=1/C_d+1/C_g$ , where  $C_d$  is the dielectric capacitance and  $C_g$  is the air gap capacitance.

In the planar configuration, the filaments make a short-circuit in the gap when the discharge occurs. Then, the total capacitance, which is equal to the capacitance of the dielectric, becomes larger.

However, in the axisymmetric configuration, the discharge occurs around the wire without making a short-circuit in the air gap. The expansion of the discharge in the gap varies with the voltage, inducing a variable gap capacitance and obviously a variable total capacitance. The slope of charge-voltage curve increases more slowly than in the planar configuration, which explains the flattening of the edges.

### B. Effect of applied voltage and frequency on discharge characteristics

Figures 5- a and 5- b show the time evolution of applied voltage, discharge current and charge-voltage curve for axisymmetric reactor when the applied voltage is  $V_{peak} = 16$  kV and the frequency is  $f = 1$  kHz.

Comparatively to figure 3 where the conditions were  $V_{peak} = 12$  kV and  $f = 1$  kHz, discharge current increases as well as the number of Trichel pulses. In addition, a glow-like discharge component appears on the negative half-cycle. The charge-voltage curve increases with the applied voltage.

Increasing the frequency at 2 kHz (figure 6- a) implies the increase of the magnitude and the number of discharge current pulses. A glow-like discharge component can also be observed during the negative half cycle. The charge-voltage curve decreases with the frequency (figure 6-b).

In the planar configuration, when the voltage is raised to  $V_{peak} = 16$  kV at fixed frequency of 1 kHz, the number of discharge current pulses increases. In addition, the charge-voltage curve increases (figure 7- a). The rise

of the frequency from 1 kHz to 2 kHz for a fixed voltage of 12 kV involves also an increase of the number of discharge current pulses.

In contrast, the charge-voltage curve remains nearly unchanged on figure 7- b compared to figure 4- c where  $V_{peak} = 12$  kV and  $f = 1$  kHz.

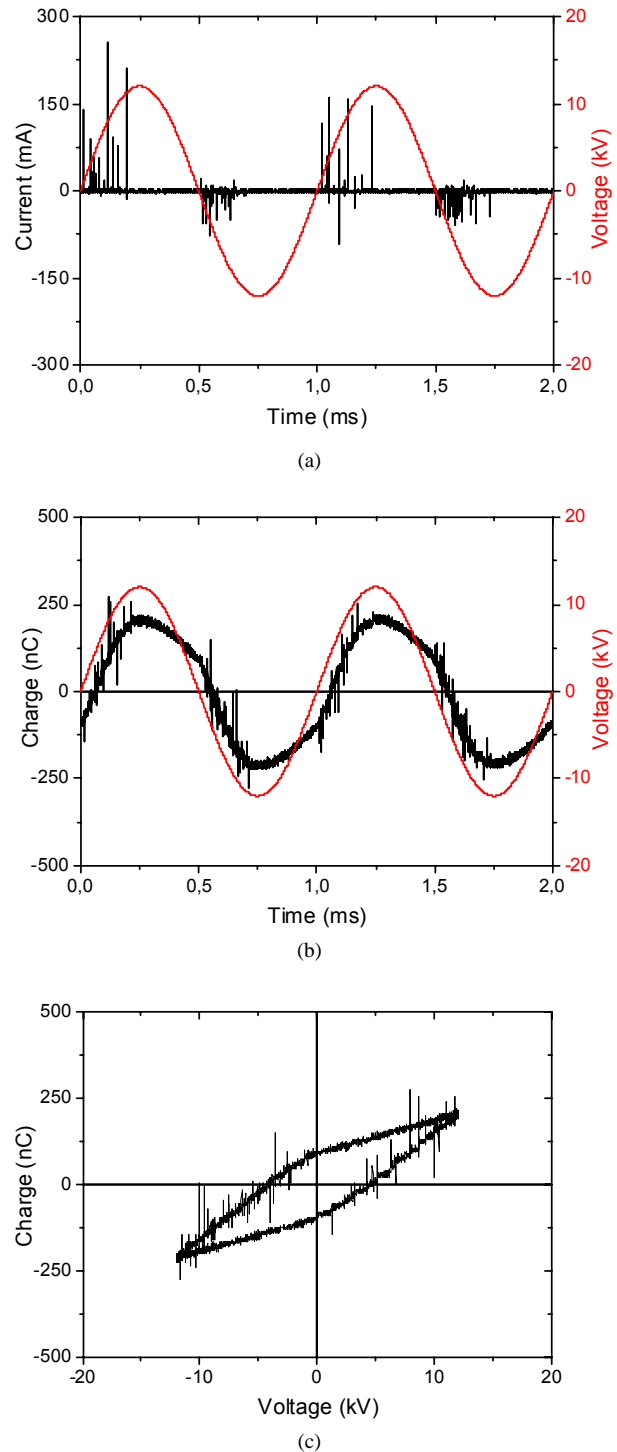


Fig. 4. Planar reactor characteristics: (a) time evolution of the discharge current, (b) time evolution of the transferred charge, and (c) charge-voltage curve. Conditions:  $V_{peak} = 12$  kV;  $f = 1$  kHz;  $Q = 4.7$  L.min<sup>-1</sup>.

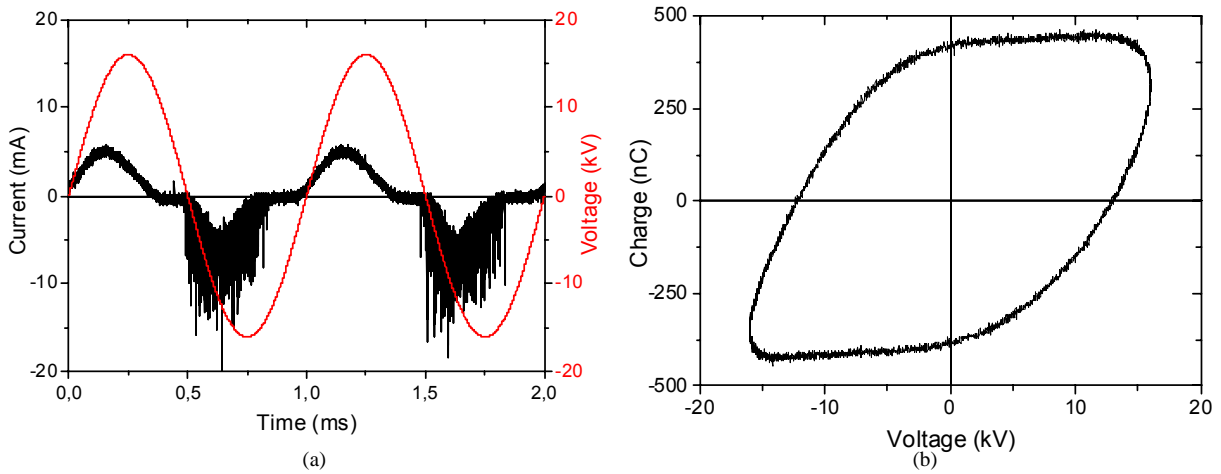


Fig. 5. (a) Time evolution of the discharge current. (b) Charge-voltage curve for axisymmetric reactor. Conditions:  $V_{\text{peak}} = 16 \text{ kV}$ ;  $f = 1 \text{ kHz}$ ;  $Q = 4.7 \text{ L}\cdot\text{min}^{-1}$ .

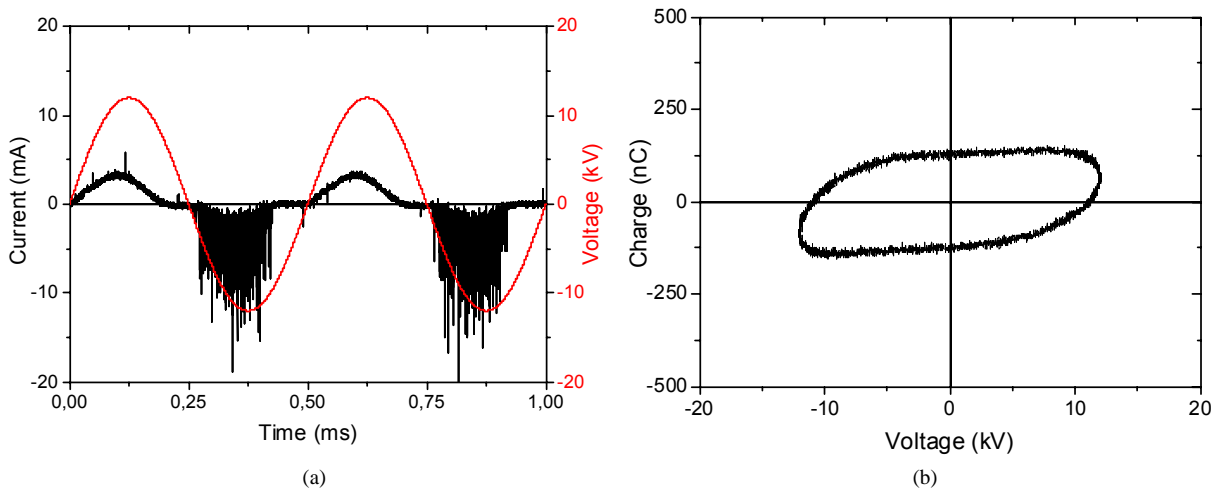


Fig. 6. (a) Time evolution of the discharge current. (b) Charge-voltage curve for axisymmetric reactor. Conditions:  $V_{\text{peak}} = 12 \text{ kV}$ ;  $f = 2 \text{ kHz}$ ;  $Q = 4.7 \text{ L}\cdot\text{min}^{-1}$ .

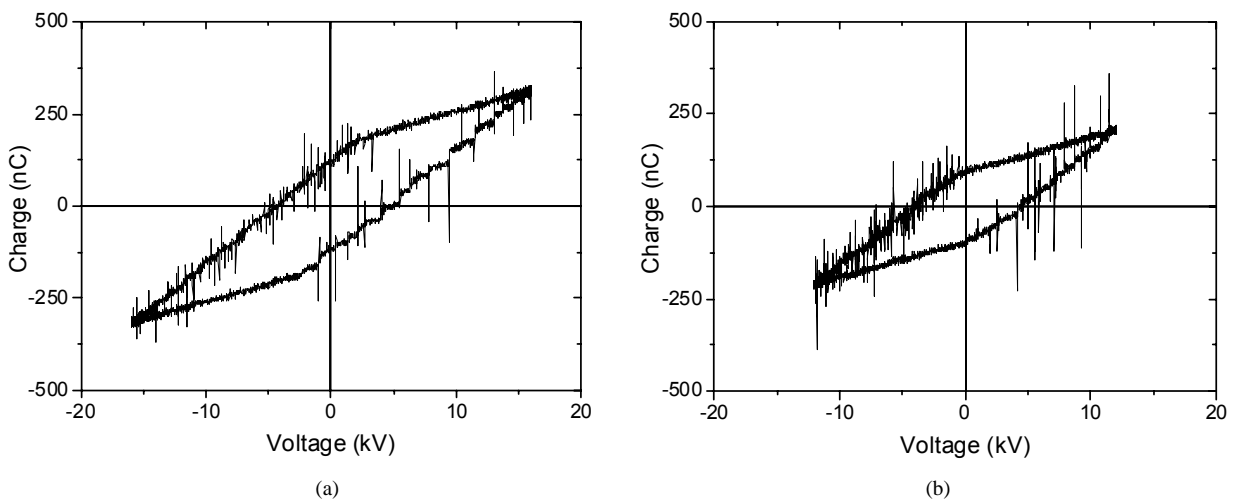


Fig. 7. Charge-voltage curve for planar reactor. (a) Conditions:  $V_{\text{peak}} = 16 \text{ kV}$ ;  $f = 1 \text{ kHz}$ ;  $Q = 4.7 \text{ L}\cdot\text{min}^{-1}$ . (b) Conditions:  $V_{\text{peak}} = 12 \text{ kV}$ ;  $f = 2 \text{ kHz}$ ;  $Q = 4.7 \text{ L}\cdot\text{min}^{-1}$ .

C. Effect of air flow on discharge characteristics

The air circulation system consists of a pressure reducing valve, a decicator containing CaSO<sub>4</sub> and a flow meter. The air used is provided by the compressed air network.

Several flow rates were applied to the discharge but only the two extreme values will be shown, i.e. 1.6 L.min<sup>-1</sup> and 15.8 L.min<sup>-1</sup>. The flow is introduced inside the reactor first, then the voltage is quickly raised up to the desired value and the discharge is maintained during one minute and finally the discharge is stopped.

Figures 8 and 9 show the waveforms of the charge-voltage curve obtained with two flow rates in the axisymmetric and planar configurations, respectively. When the flow rate is increased, the discharge current decreases and the ignition voltage of the discharge increases (figure 10). Consequently, with higher flow rates the transferred charge is lower. This effect is more pronounced in the axisymmetric configuration.

The effect of the flow rate on the average power is shown on figure 11. The flow rate varies between 1.6 and

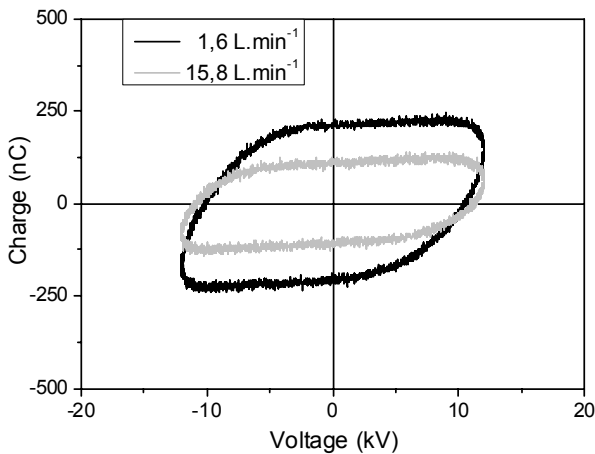


Fig. 8. Charge-voltage curve for axisymmetric reactor. Conditions: V<sub>peak</sub> = 12 kV; f = 1 kHz.

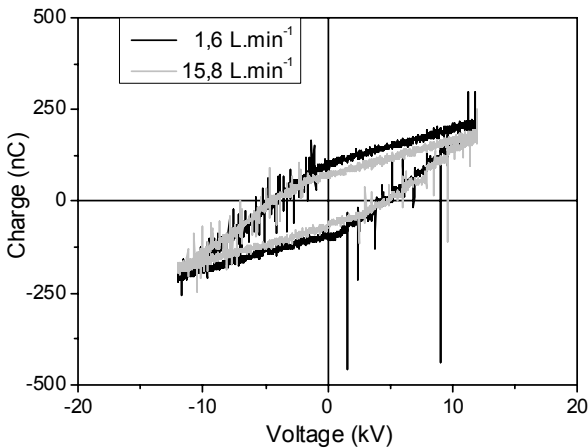


Fig. 9. Charge-voltage curve for planar reactor, Conditions: V<sub>peak</sub> = 12 kV; f = 1 kHz.

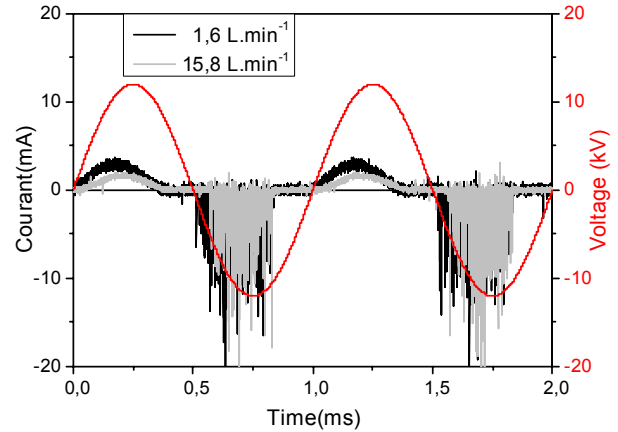


Fig. 10. Axisymmetric reactor characteristics: time evolution of the discharge current. Conditions: V<sub>peak</sub> = 12 kV; f = 1 kHz.

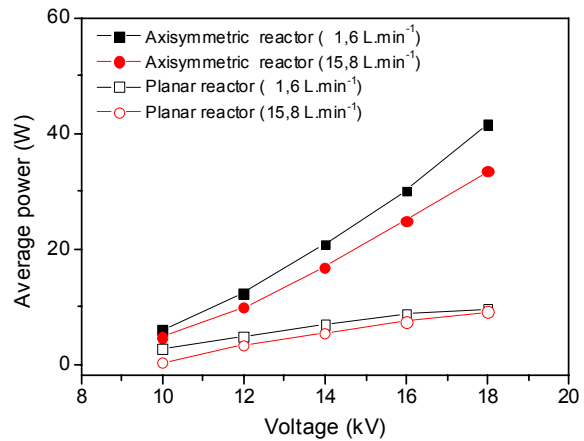


Fig. 11. Average power/voltage curve for axisymmetric and planar reactors at f = 1 kHz.

15.8 L.min<sup>-1</sup>. A high flow rate induces a low average power for both reactors. However, this tendency is more important with the axisymmetric reactor than the planar one.

During the discharge, it seems that some charges are transported outside the plasma section because of the airflow. This phenomenon is pronounced at high flow rates and explains the result shown in figures 8-11. In addition, the streamers at the origin of the filamentary discharge progress rapidly in the gap (about 10 ns). Thus, the filamentary discharge is not very affected by the velocity of the air (some m/s).

IV. CONCLUSION

The characteristics of the Dielectric Barrier Discharge in axisymmetric and planar configurations are studied and compared by measuring their electrical discharge parameters and the airflow influence on these parameters.

It was observed that the DBD discharge characteristics in axisymmetric configuration are different from those of the planar configuration. By modifying the geometry of the reactors, a different discharge type can be obtained using the same electric excitation.

In axisymmetric configuration, DBD discharge is rather quasi-diffuse while, in the planar one, the discharge is filamentary.

The study of the influence of the air flow on the discharge show that discharge current, transferred charge and average power decrease with the flow rate. This evolution is more pronounced with the axisymmetric reactor.

Now, both reactors are going to be tested for particle precipitation, agglomeration or destruction.

#### REFERENCES

- [1] F. S. Denes and S. Manolache, "Macromolecular plasma-chemistry: an emerging field of polymer science", *Prog. Polym. Sci.*, Vol. 29, No.8, pp. 815-885, August 2004.
- [2] N. Gherardi and F. Massines, "Mechanisms controlling the transition from glow silent discharge to streamers discharge in nitrogen", *IEEE Trans. Plasma Sci.*, Vol. 29, No.3, pp. 536-544, 2001.
- [3] J. H. Byeon, J. Hwang, J. H. Park, K. Y. Yoon, B. J. Ko, S. H. Kang and J. H. Ji, "Collection of submicron particles by an electrostatic precipitator using a dielectric barrier discharge", *J. Aerosol Sci.*, Vol. 37, pp. 1618-1628, November 2006.
- [4] S. Sato, M. Kimura, T. Aki, I. Koyamoto, K. Takashima, S. Katsua and A. Mizuno, "Removal of diesel particles using an electrostatic precipitator with a barrier discharge electrode as a dust pocket", *Proc. ESA/IEJ/IEEE-IAS/SFE joint Conference on Electrostatics 2006, Berkley California*, pp. 754-762, 6-9 June, 2006.
- [5] Y. Dan, G. Dengshan, Y. Gang, S. Xianglin and G. Fan, "An investigation of the treatment of particulate matter from gasoline engine exhaust using non-thermal plasma", *J. Hazard. Mater.*, Vol. B127, pp. 149-155, December 2005.
- [6] Z. Fang, Y. Qiu, C. Zhang, and Kuffel, "Factors influencing the existence of the homogeneous dielectric barrier discharge in air at atmospheric pressure", *J. Phys. D: Appl. Phys.*, Vol. 40, pp. 1401-1407, February 2007.
- [7] J. R. Roth, J. Rahel, X. Dai and D. M. Sherman, "The physics and phenomenology of One Atmosphere Uniform Glow Discharge Plasma (OAUGDP™) reactor for surface treatment applications", *J. Phys. D: Appl. Phys.*, Vol. 38, pp. 555-567, February 2005.
- [8] J. Rahel and D. M. Sherman, "The transition from a filamentary dielectric barrier discharge to a diffuse barrier discharge in air at atmospheric pressure", *J. Phys. D: Appl. Phys.*, vol. 38, pp. 547-554, February 2005.
- [9] M. Abdel-Salam, A. Hashem, A. Yehia, A. Mizuno, A. Turkey and A. Gabr, "Characteristics of corona and silent discharges as influenced by geometry of the discharge reactor", *J. Phys. D: Appl. Phys.*, Vol. 36, pp. 252-260, January 2003.
- [10] M. Petit, A. Goldman and M. Goldman, "Glow currents in a point-to-plane dielectric barrier discharge in the context of the chemical reactivity control", *J. Phys. D: Appl. Phys.*, Vol. 35, pp. 2969-2977, November 2002.
- [11] I. Nagao, M. Nishida, K. Yukimura, S. Kambara and T. Maruyama, "NO<sub>x</sub> removal using nitrogen gas activated by dielectric barrier discharge at atmospheric pressure", *Vacuum*, Vol. 65, No. 3-4, pp. 481-487, May 2002.